Available online at www.sciencedirect.com
SCIENCE DIRECT®
ELSEVIER
International Journal of Solids and Structures 42 (2005) 1187–1207
INTERNATIONAL JOURNAL OF SOLIDS and STRUCTURES
www.elsevier.com/locate/ijsolstr

Stability of a two-mass oscillator moving on a beam supported by a visco-elastic half-space

A.V. Metrikine *, S.N. Verichev, J. Blaauwendraad

Faculty of Civil Engineering and Geosciences, Delft University of Technology, P.O. Box 5048, 2600 GA Delft, The Netherlands

Received 13 December 2003; received in revised form 5 March 2004
Available online 24 August 2004

Abstract

This paper presents a theoretical study of the stability of a two-mass oscillator that moves along a beam on a visco-elastic half-space. The oscillator and the beam on the half-space are employed to model a bogie of a train and a railway track, respectively. Using Laplace and Fourier integral transforms, expressions for the dynamic stiffness of the beam are derived in the point of contact with the oscillator. It is shown that the imaginary part of this stiffness can be negative thereby corresponding to so-called negative damping. This damping can destabilize the oscillator leading to the exponential growth of the oscillator's displacement. The instability zone corresponding to such behavior is found in the space of the system's parameters with the help of the D-decomposition method. A parametric study of this zone is carried out with the emphasis on the effect of the material damping in the half-space and the viscous damping in the oscillator. It is shown that a proper combination of these damping mechanisms stabilizes the system effectively. An attempt is made to construct a one-dimensional foundation of the beam so that the instability zone predicted by the resulting one-dimensional model would coincide with that obtained from the original three-dimensional model. It is shown that such foundation can be constructed but its parameters are ambiguous and cannot be determined a-priori, without tuning the instability zone. Therefore, it is concluded that one-dimensional models should not be used for the stability analysis of high-speed trains.

1. Introduction

The operational speed of modern high-speed trains is so high that the dynamic effects become important, which were of no significance for conventional railways. Among these effects is the dynamic train–rail–soil interaction. Considering this interaction, researchers employ various models, which differ by complexity of one or more components of the train–rail–soil system. A comprehensive review of these models is presented by Popp et al. (1999).

In almost all studies on the issue it is implicitly assumed that there exists the steady-state regime of the interaction. This means that after a sufficiently long time the system's vibrations are assumed to become

* Corresponding author. Tel.: + 31-15-2784749; fax: + 31-15-2785767.
E-mail address: a.metrikine@citg.tudelft.nl (A.V. Metrikine).

0020-7683/$ - see front matter © 2004 Elsevier Ltd. All rights reserved.
doi:10.1016/j.ijsolstr.2004.03.006

independent of the initial conditions and the dynamic behavior to become repetitive or quasi-repetitive, depending on the applied forces and the railway track's regularity. This assumption is fully justified if the train is modeled by a system of a priori prescribed forces and no degrees of freedom of the train are accounted for, see Filippov (1961), Labra (1975), Krylov (1995), Dieterman and Metrikine (1997), Grundmann et al. (1999), Sheng et al. (1999), Kaynia et al. (2000), Andersen and Nielsen (2003a), Vostroukhov and Metrikine (2003). On the contrary, if the train is described as a single- or multi-degree of freedom system, the motion of the train may be unstable and the steady-state regime may be not reachable.

The instability of a moving object on an elastic structure was first described by Denisov et al. (1985) and Bogacz et al. (1986). In these papers, it was shown that if the objects speed exceeded the minimum phase velocity of waves in the elastic structure, the object's motion might become unstable. Metrikine (1994) showed that the energy needed for the instability is supplied by the external source, which maintains the object's motion along the structure.

During the last decade, several papers were published devoted to the instability. All these papers (Metrikine and Vesnitsky, 1996; Metrikine and Dieterman, 1997a; Zheng et al., 2000; Metrikine and Verichev, 2001; Kononov and de Borst, 2002; Zheng and Fan, 2002; Verichev and Metrikine, 2000, 2002, 2003) but one of Metrikine and Popp (1999) dealt with one-dimensional models of the railway track. Because of the one-dimensional modeling, these studies cannot be used for quantitative prediction of the train-track stability but they convey an important message that the stability is not guaranteed at high speeds. Moreover, as shown by Metrikine and Vesnitsky (1996) and Verichev and Metrikine (2003), because of the track inhomogeneity the train can loose its stability at low speeds because of parametric resonance. Such instability could arise, for example, in the models, which have been recently studied by Andersen et al. (2002) and Andersen and Nielsen (2003b).

Since the models of the train-track dynamic interaction become more complicated and tend to account for the train in a realistic manner, e.g. as for a single- or multi-degree of freedom system (Clouteau et al., 2001; Grundmann and Lenz, 2003), the stability issue has to be discussed in more detail.

The main aim of this paper is to carry out a parametric study of the stability of a three-dimensional model of the train–track interaction, which accounts for the dissipation mechanisms both in the ground and in the train's suspension system. The emphasis of the study is placed on the effect of the amount of damping on the train's stability.

The model under consideration consists of a two-mass oscillator and a beam on a visco-elastic half-space, which are employed to model a train's bogie and the rail–soil structure, respectively. The assumptions with which the model is studied are described in the next section.

Since the model under consideration is linear, the study is accomplished with the help of Laplace and Fourier integral transforms, which allow for obtaining the characteristic equation for the vertical motion of the oscillator. The roots of this equation (the eigenvalues) are analyzed employing the D-decomposition method (Neimark, 1978). The combinations of parameters, which correspond to at least one eigenvalue with a positive real part, form the instability domain in the space of the model parameters. The effect of the system's parameters on this domain is studied thoroughly, with the emphasis on the effect of the damping mechanisms.

The paper is concluded with a discussion on capabilities of one-dimensional models to predict the stability of high-speed trains correctly.

2. The model and the governing equations

The model under consideration is composed of a two-mass oscillator, an infinitely long beam of a finite width, and a visco-elastic half-space, as depicted in Fig. 1. The oscillator vibrates vertically and moves

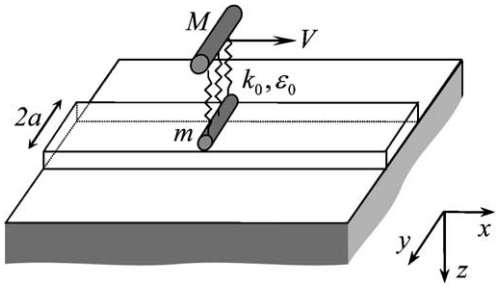

Fig. 1. The model and the reference system.

uniformly along the beam, which is supported by the half-space. The aim of this paper is to study the stability of small vertical motion of the oscillator as it remains in contact with the beam.

The following assumptions concerning the beam, the half-space and their contact are accepted in this study (Metrikine et al., 2001):

- The beam has a finite width $2a$, is infinitely stiff in the lateral (y) direction, and the Euler–Bernoulli model describes its vertical motion.
- The visco-elastic half-space is isotropic, homogeneous, and made of a material that satisfies the phenomenological Kelvin–Voigt model.
- The contact between the beam and the half-space is modeled approximately so that
  - the surface tractions σ_{zz} and σ_{xz} are uniformly distributed beneath the beam;
  - the vertical displacement of the beam is equal to the vertical displacement of the half-space surface along the line $y = 0$;
  - the lateral surface traction σ_{yz} is neglected, since with the above formulated assumptions this traction does not influence the vertical motion of the beam (Metrikine and Dieterman, 1997b).
  - The shear contact in the x-direction between the beam and the half-space is considered as depicted in Fig. 2, which presents the vertical cross-section of the system by the plane $y = 0$ (see also Metrikine et al., 2001). This figure shows that this contact takes place through shear springs with the stiffness per unit length K, which are uniformly and continuously distributed beneath the beam. The upper ends of the springs are immovable in the x-direction whereas the lower ends undergo a displacement equal to the horizontal displacement of the half-space surface along the centerline of the beam.

  With these assumptions, equations that govern small vibrations of the system can be written as follows:
- the equations of motion of the half-space in terms of the scalar and vector potentials φ and $\boldsymbol{\psi} = \boldsymbol{x}_0\psi^x + \boldsymbol{y}_0\psi^y + \boldsymbol{z}_0\psi^z$:

$$\hat{c}_L^2\nabla^2\varphi = \partial_{tt}\varphi, \qquad \hat{c}_T^2\nabla^2\boldsymbol{\psi} = \partial_{tt}\boldsymbol{\psi}, \qquad \nabla \bullet \boldsymbol{\psi} = 0, \tag{1}$$

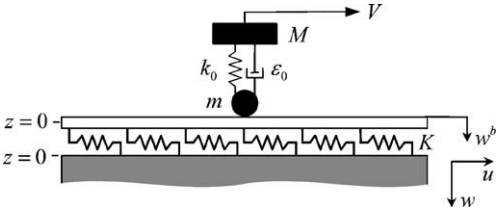

Fig. 2. The vertical cross-section $y = 0$ with enlarged interface between the beam and the half-space.

where $\hat{c}_L^2 = (\hat{\lambda} + 2\hat{\mu})/\rho$, $\hat{c}_T^2 = \hat{\mu}/\rho$, ρ is the mass density, ∂_t is the partial time derivative and $\nabla = x_0\partial_x + y_0\partial_y + z_0\partial_z$ is the Nabla operator in which ∂_x, ∂_y and ∂_z are the partial derivatives with respect to x, y and z, respectively. $\hat{\lambda} = \lambda + \lambda^*\partial_t$ and $\hat{\mu} = \mu + \mu^*\partial_t$ are operators that are applied instead of the Lamé constants to describe the visco-elastic material of the half-space in accordance with the Kelvin–Voigt model.

- the balance of stresses at the surface of the half-space $z = 0$:

$$\begin{aligned}
\sigma_{zz}(t,x,y,0) &= \frac{1}{2a}H(a-|y|)((m_b\partial_{tt} + EI\partial_{xxxx})w^b + \delta(x-Vt)(md_{tt}w^{01} + (k_0+\varepsilon_0 d_t)(w^{01}-w^{02})))\\
\tau_{xz}(t,x,y,0) &= \frac{1}{2a}H(a-|y|)Ku(t,x,0,0),\\
\tau_{yz}(t,x,y,0) &= 0,
\end{aligned} \tag{2}$$

  where $w^b(t,x)$, $w^{01}(t)$ and $w^{02}(t)$ are the vertical displacements of the beam and the masses of the oscillator m and M, respectively, $u(t,x,y,z)$ is the displacement of the half-space in the x-direction, m_b and EI are the mass per unit length and the bending stiffness of the beam, k_0 and ε_0 are the stiffness and the viscosity of the oscillator, K is the stiffness of the shear springs, $\delta(\ldots)$ and $H(\ldots)$ are the Dirac delta function and the Heaviside step function, d_t is the time derivative, ∂_x is the partial derivative over x;
- the continuity of vertical displacements of the beam and the half-space:

$$w(t,x,0,0) = w^b(t,x) \tag{3}$$

  with $w(t,x,y,z)$ the half-space displacement in the z-direction;
- the continuity of vertical displacements of the lower mass of the oscillator and the beam:

$$w^{01}(t) = w^b(t,x)_{x=Vt}; \tag{4}$$

- the equation of the vertical motion of the upper mass of the oscillator:

$$Md_{tt}w^{02} + (k_0+\varepsilon_0 d_t)(w^{02}-w^{01}) = 0. \tag{5}$$

To analyze the model, we will follow the approach proposed by Metrikine and Popp (1999). In accordance with this approach, firstly, the equations of motion are transformed into the reference system that moves along the x-direction with the velocity of the oscillator. Secondly, the Laplace transform over time and the integral Fourier transform over the new longitudinal coordinate are applied. Then, an equivalent stiffness $\chi_{eq}^{h\text{-}s}(\omega,k_1)$ of the half-space is calculated as a complex function of the frequency ω and wavenumber k_1 of the bending waves in the beam. Introduction of this stiffness will reduce the original 3D model to an equivalent 1D model, in which the beam is supported by an equivalent foundation with the stiffness $\chi_{eq}^{h\text{-}s}(\omega,k_1)$ as shown in Fig. 3. Note that no additional assumption is needed for this reduction since $\chi_{eq}^{h\text{-}s}(\omega,k_1)$ can describe the half-space reaction to any beam motion.

The next step is to reduce the model further by calculating the equivalent stiffness $\chi_{eq}^{beam}(\omega,V)$ of the beam in the point of contact with the moving oscillator. This stiffness is the dynamic complex stiffness of the beam, which depends on the frequency of the oscillator's vibrations and on the velocity of its motion along the beam. As shown by Metrikine and Popp (1999) and Metrikine and Verichev (2001), the imaginary part of this stiffness determines whether the oscillator may be unstable. With the equivalent stiffness of the beam $\chi_{eq}^{beam}(\omega,V)$, the model reduces further to a well-known lumped model depicted in Fig. 4. Thus, to obtain the characteristic equation for the vertical motion of the oscillator, whose roots determine the system's stability, we need to find $\chi_{eq}^{beam}(\omega,V)$.

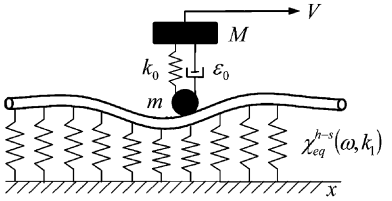

Fig. 3. Equivalent 1D model for the beam-oscillator coupled motion. The reaction of the half-space is accounted for by the foundation with complex stiffness $\chi_{\mathrm{eq}}^{\mathrm{h\text{-}s}}(\omega,k_1)$.

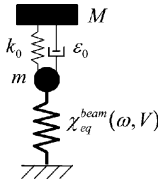

Fig. 4. Equivalent lumped model for the vertical motion of the oscillator. The reaction of the beam-half-space system is given by the equivalent spring with complex stiffness $\chi_{\mathrm{eq}}^{\mathrm{beam}}(\omega,V)$.

Let us accomplish the above-described steps. Firstly, a moving reference system is introduced, which is defined as

$$\begin{cases} \xi = x - Vt, \quad y = y, \quad z = z, \\ \tau = t. \end{cases} \tag{6}$$

Transforming the problem statement given by Eqs. (1)–(5) into this reference system gives a system of equations (A.1)–(A.5), that is presented in Appendix A.

Secondly, the Laplace transform with respect to time and the integral Fourier transforms with respect to the horizontal co-ordinates ξ and y are applied to Eqs. (A.1)–(A.5). These transforms are defined as

$$f_{s,k_1,k_2}(s,k_1,k_2) = \int_0^\infty \int_{-\infty}^\infty \int_{-\infty}^\infty f(\tau,\xi,y)\exp(-st - \mathrm{i}(k_1\xi + k_2 y))\mathrm{d}\xi\,\mathrm{d}y\,\mathrm{d}\tau. \tag{7}$$

The resulting system of equations in the Laplace-Fourier domain reads

- equations of motion of the half-space:

$$\begin{aligned} &\left(\tilde{c}_L^2(\partial_{zz} - k_1^2 - k_2^2) - (s - \mathrm{i}k_1 V)^2\right)\varphi_{s,k_1,k_2} = 0, \\ &\left(\tilde{c}_T^2(\partial_{zz} - k_1^2 - k_2^2) - (s - \mathrm{i}k_1 V)^2\right)\boldsymbol{\psi}_{\boldsymbol{s,k_1,k_2}} = 0, \end{aligned} \tag{8}$$

$$\mathrm{i}k_1\psi^{\xi}_{s,k_1,k_2} + \mathrm{i}k_2\psi^{y}_{s,k_1,k_2} + \partial_z\psi^{z}_{s,k_1,k_2} = 0 \tag{9}$$

with $\tilde{c}_L^2 = (\lambda_{s,k_1} + 2\mu_{s,k_1})/\rho$, $\tilde{c}_T^2 = \mu_{s,k_1}/\rho$, and $\lambda_{s,k_1} = \lambda + (s - \mathrm{i}k_1 V)\lambda^*$ and $\mu_{s,k_1} = \mu + (s - \mathrm{i}k_1 V)\mu^*$,

- the balance of stresses at $z = 0$ (employing the expressions for stresses given by Eq. (A.7)):

$$
\begin{aligned}
&\left(\lambda_{s,k_1}(\partial_{zz}-k_1^2-k_2^2)\varphi_{s,k_1,k_2}+2\mu_{s,k_1}(\partial_{zz}\varphi_{s,k_1,k_2}+\mathrm{i}\partial_z(k_1\psi^y_{s,k_1,k_2}-k_2\psi^{\xi}_{s,k_1,k_2}))\right)_{z=0}\\
&\qquad=\left(w^{\mathrm{b}}_{s,k_1}D_{s,k_1}+ms^2w^{01}_{\mathrm{s}}+(k_0+s\varepsilon_0)(w^{01}_{\mathrm{s}}-w^{02}_{\mathrm{s}})\right)\frac{\sin(k_2a)}{k_2a},\\
&\mu_{s,k_1}\left(2\mathrm{i}k_1\partial_z\varphi_{s,k_1,k_2}+\mathrm{i}k_2\partial_z\psi^z_{s,k_1,k_2}-\partial_{zz}\psi^y_{s,k_1,k_2}-k_1^2\psi^y_{s,k_1,k_2}+k_1k_2\psi^{\xi}_{s,k_1,k_2}\right)_{z=0}\\
&\qquad=Ku_{s,k_1}(s,k_1,y,z)_{y=0,z=0}\frac{\sin(k_2a)}{k_2a},\\
&\mu_{s,k_1}\left(2\mathrm{i}k_2\partial_z\varphi_{s,k_1,k_2}+\partial_{zz}\psi^{\xi}_{s,k_1,k_2}-\mathrm{i}k_1\partial_z\psi^z_{s,k_1,k_2}-k_1k_2\psi^y_{s,k_1,k_2}+k_2^2\psi^{\xi}_{s,k_1,k_2}\right)_{z=0}\\
&\qquad=0,
\end{aligned}
\tag{10}
$$

with $D_{s,k_1}=m_{\mathrm{b}}(s-\mathrm{i}k_1V)^2+EIk_1^4$,

- the continuity of vertical displacements of the beam and the half-space:

$$
w^{\mathrm{b}}_{s,k_1}(s,k_1)=w_{s,k_1}(s,k_1,y,z)_{y=0,z=0}=\frac{1}{2\pi}\int_{-\infty}^{\infty}w_{s,k_1,k_2}(s,k_1,k_2,z)_{z=0}dk_2, \tag{11}
$$

since $\exp(\mathrm{i}k_2y)_{y=0}=1$,

- the continuity of vertical displacements of the lower mass of the oscillator and the beam:

$$
w^{01}_{\mathrm{s}}(s)=w^{\mathrm{b}}_{\mathrm{s}}(s,\xi)_{\xi=0}, \tag{12}
$$

- the equation of the vertical motion of the upper mass of the oscillator:

$$
Ms^2w^{02}_{\mathrm{s}}+(k_0+\varepsilon_0s)(w^{02}_{\mathrm{s}}-w^{01}_{\mathrm{s}})=0. \tag{13}
$$

The general solution to Eq. (8), requiring that φ_{s,k_1,k_2} and $\boldsymbol{\psi}_{s,k_1,k_2}$ vanish at $z\to\infty$, is

$$
\begin{aligned}
&\varphi_{s,k_1,k_2}=A\exp(-zR_L),\qquad \psi^{\xi}_{s,k_1,k_2}=B_{\xi}\exp(-zR_T),\\
&\psi^{y}_{s,k_1,k_2}=B_{y}\exp(-zR_T),\qquad \psi^{z}_{s,k_1,k_2}=B_{z}\exp(-zR_T),\\
&R_{L,T}=\sqrt{k_1^2+k_2^2+(s-\mathrm{i}k_1V)^2/\tilde{c}^2_{L,T}}
\end{aligned}
\tag{14}
$$

provided that the branches of the square roots in the complex domain are chosen such that $\mathrm{Re}(R_{L,T})>0$.

Substituting Eqs. (14) into (9) the boundary conditions Eq. (10) the following system of linear algebraic equations with respect to unknowns A, B_{ξ}, B_y and B_z is obtained:

$$
\begin{array}{ccccccccc}
 & & \mathrm{i}k_1B_{\xi} & + & \mathrm{i}k_2B_y & - & R_TB_z & = & 0,\\
-2\mathrm{i}k_1R_LA & + & k_1k_2B_{\xi} & + & (-R_T^2-k_1^2)B_y & + & (-\mathrm{i}k_2R_T)B_z & = & H_{\xi},\\
-2\mathrm{i}k_2R_LA & + & (R_T^2+k_2^2)B_{\xi} & + & (-k_1k_2)B_y & + & (\mathrm{i}k_1R_T)B_z & = & 0,\\
\left(2(k_1^2+k_2^2)+\dfrac{(s-\mathrm{i}k_1V)^2}{\tilde{c}_T^2}\right)A & + & 2\mathrm{i}k_2R_TB_{\xi} & + & (-2\mathrm{i}k_1R_T)B_y & & & = & H_z
\end{array}
\tag{15}
$$

with

$$
\begin{cases}
H_x=Ku_{s,k_1}(s,k_1,0,0)\sin k_2a/(\tilde{\mu}_{s,k_1}k_2a)\\
H_z=\left(w^{b}_{s,k_1}D_{s,k_1}+ms^2u^{01}_{s}+(k_0+s\varepsilon_0)(w^{01}_{s}-w^{02}_{s})\right)\sin k_2a/(\tilde{\mu}_{s,k_1}k_2a).
\end{cases}
\tag{16}
$$

Eq. (15) can be readily solved to give

$$A = \frac{\Delta_A}{\Delta_0}, \qquad B_\xi = \frac{\Delta_{B_\xi}}{\Delta_0}, \qquad B_y = \frac{\Delta_{B_y}}{\Delta_0}, \qquad B_x = \frac{\Delta_{B_z}}{\Delta_0}, \tag{17}$$

with determinants Δ_0, Δ_A, Δ_{B_ξ}, Δ_{B_y}, Δ_{B_z} defined in Appendix B.

Now, we need to determine the Laplace–Fourier displacements of the half-space surface in the x- and z- directions. In accordance with Eq. (A.6), these displacements read (zero in the arguments corresponds to $z = 0$)

$$\begin{aligned} u_{s,k_1,k_2}(s,k_1,k_2,0) &= (\mathrm{i}k_1\varphi_{s,k_1,k_2} + \mathrm{i}k_2\psi^z_{s,k_1,k_2} - \partial_z\psi^y_{s,k_1,k_2})_{z=0} = \mathrm{i}k_1 A + \mathrm{i}k_2 B_z + R_T B_y, \\ w_{s,k_1,k_2}(s,k_1,k_2,0) &= \left(\partial_z\varphi_{s,k_1,k_2} + \mathrm{i}k_1\psi^y_{s,k_1,k_2} - \mathrm{i}k_2\psi^\xi_{s,k_1,k_2}\right)_{z=0} = -R_L A + \mathrm{i}k_1 B_y + \mathrm{i}k_2 B_\xi. \end{aligned} \tag{18}$$

Substitution of Eq. (17) into Eq. (18) gives

$$\begin{aligned} u_{s,k_1,k_2}(s,k_1,k_2,0) &= a_{11}H_\xi + a_{13}H_z, \\ w_{s,k_1,k_2}(s,k_1,k_2,0) &= a_{31}H_\xi + a_{33}H_z \end{aligned} \tag{19}$$

with

$$a_{11} = \frac{1}{R_T\Delta}\left(2k_1^2R_T^2 - (R_T^2 + k_2^2)q + 4k_2^2R_LR_T\right), \qquad a_{13} = \frac{\mathrm{i}k_1}{\Delta}(q - 2R_LR_T),$$

$$a_{31} = -a_{13}, \qquad a_{33} = -\frac{(s - \mathrm{i}k_1V)^2}{\tilde{c}_T^2}\frac{R_L}{\Delta}, \qquad \Delta = \frac{\Delta_0\tilde{c}_T^2}{(s - \mathrm{i}k_1V)^2R_T}.$$

Application of the inverse Fourier transform with respect to k_2 to Eq. (19) followed by substitution of Eq. (16) yields

$$\begin{aligned} u_{s,k_1}(s,k_1,0,0) &= \frac{K}{2\pi\mu_{s,k_1}}I_{11}u_{s,k_1} + \frac{I_{13}}{2\pi\mu_{s,k_1}}\left(w^{\mathrm{b}}_{s,k_1}D_{s,k_1} + ms^2w_{\mathrm{s}}^{01} + (k_0 + s\varepsilon_0)(w_{\mathrm{s}}^{01} - w_{\mathrm{s}}^{02})\right), \\ w_{s,k_1}(s,k_1,0,0) &= \frac{K}{2\pi\mu_{s,k_1}}I_{31}u_{s,k_1} + \frac{I_{33}}{2\pi\mu_{s,k_1}}(w^{\mathrm{b}}_{s,k_1}D_{\mu_{s,k_1}} + ms^2w_{\mathrm{s}}^{01} + (k_0 + s\varepsilon_0)(w_{\mathrm{s}}^{01} - w_{\mathrm{s}}^{02})), \\ I_{ij} &= \int_{-\infty}^{+\infty} a_{ij}\frac{\sin(ak_2)}{ak_2}dk_2, \quad i,j = 1,3. \end{aligned} \tag{20}$$

Eliminating u_{s,k_1} from Eq. (20) and using the continuity condition Eq. (11) the following equation for the Laplace–Fourier vertical displacement of the beam can be obtained:

$$w^{\mathrm{b}}_{s,k_1}(\chi^{\text{h-s}}_{\mathrm{eq}}(s,k_1) + D_{s,k_1}) = -w_{\mathrm{s}}^{01}(ms^2 + k_0 + \varepsilon_0 s) + w_{\mathrm{s}}^{02}(k_0 + \varepsilon_0 s), \tag{21}$$

where

$$\chi^{\text{h-s}}_{\mathrm{eq}}(s,k_1) = \frac{2\pi\mu_{s,k_1}(2\pi\mu_{s,k_1} - KI_{11})}{(KI_{11} - 2\pi\mu_{s,k_1})I_{33} - KI_{13}^2} \tag{22}$$

is the equivalent dynamic stiffness of the half-space.

Eq. (21), accompanied by the equation of motion of the upper mass of the oscillator, Eq. (13) and the continuity condition between the lower mass of the oscillator and the beam, Eq. (12) describes vibrations of the oscillator on the beam supported by an equivalent foundation as depicted in Fig. 3. The stiffness of this foundation $\chi^{\text{h-s}}_{\mathrm{eq}}$ is a complex-valued function of the Laplace parameter s and the wavenumber k_1.

Thus, the first step of the model reduction has been made—the model has been reduced to an equivalent one-dimensional model. The next step is to obtain an equivalent lumped model depicted in Fig. 4. To carry

out this step, the inverse Fourier-transform over k_1 is applied to Eq. (21). With the help of the continuity condition Eq. (12), the following equation is obtained:

$$w^{01}(ms^2 + k_0 + \varepsilon_0 s + \chi_{\text{eq}}^{\text{beam}}(s)) - w^{02}(k_0 + \varepsilon_0 s) = 0, \tag{23}$$

where

$$\chi_{\text{eq}}^{\text{beam}}(s) = \left(\frac{1}{2\pi} \int_{-\infty}^{\infty} \frac{\mathrm{d}k_1}{\chi_{\text{eq}}^{\text{h-s}}(s, k_1) + D_{s,k_1}} \right)^{-1}. \tag{24}$$

The expression for $\chi_{\text{eq}}^{\text{beam}}$ determines the equivalent dynamic stiffness of the beam on the half-space at the contact point with the moving oscillator.

Eqs. (23) and (13) describe the dynamic system depicted in Fig. 3. Thus, the original 3D model has been reduced (exactly) to an equivalent lumped model with a complex stiffness element $\chi_{\text{eq}}^{\text{beam}}$. Now that this goal has been reached, the characteristic equation for the vertical vibrations of the oscillator can be obtained readily. In accordance with Eqs. (23) and (13) this characteristic equation reads

$$(ms^2 + k_0 + s\varepsilon_0 + \chi_{\text{eq}}^{\text{beam}}(s))(Ms^2 + k_0 + s\varepsilon_0) - (k_0 + s\varepsilon_0)^2 = 0. \tag{25}$$

The characteristic equation (25) looks exactly the same as that obtained by Metrikine and Verichev (2001) for an oscillator moving on Timoshenko beam supported by a Kelvin foundation (one dimensional visco-elastic foundation). However, the dynamic stiffness of the beam $\chi_{\text{eq}}^{\text{beam}}$ (s) in Eq. (25) and that in the paper of Metrikine and Verichev (2001) are different functions. The former dynamic stiffness is much more complicated since, in accordance with Eq. (24) it depends on the dynamic stiffness of the half-space $\chi_{\text{eq}}^{\text{h-s}}(s, k_1)$, whereas the complex stiffness of the Kelvin foundation is given by $\chi_{\text{Kelvin}} = K_0 + sC_0$ with constant K_0 and C_0. The difference between $\chi_{\text{eq}}^{\text{h-s}}(s, k_1)$ and χ_{Kelvin} is discussed in detail in papers of Dieterman and Metrikine (1996) and Metrikine and Popp (1999).

3. Equivalent dynamic stiffness of the beam

As shown by Metrikine and Dieterman (1997a), Metrikine and Popp (1999) and Verichev and Metrikine (2000), the stability of an oscillator, which moves on a beam depends crucially on the dynamic stiffness $\chi_{\text{eq}}^{\text{beam}}$ (s) of the beam in the moving contact point. More precisely, it is the imaginary part of the dynamic stiffness that determines whether the oscillator may be unstable. The instability may arise only in the case that the imaginary part of $\chi_{\text{eq}}^{\text{beam}}$ (s) is negative at a frequency band.

Thus, it is worth to start the stability analysis by studying the dynamic stiffness $\chi_{\text{eq}}^{\text{beam}}$ (s). This stiffness depends on the Laplace variable s, which is, in general, a complex value. However, as shown by Metrikine and Dieterman (1997a), if the D-decomposition method (Neimark, 1978; Denisov et al., 1985; Metrikine and Dieterman, 1997a) is employed for the stability analysis, it is sufficient to consider $s = \mathrm{i}\omega$, $\omega \in \mathbb{R}$, where ω has the sense of the radial frequency of the oscillator's vertical vibration. Substitution $s = \mathrm{i}\omega$ into Eq. (24) gives the following expression, which will be studied in this section numerically:

$$\chi_{\text{eq}}^{\text{beam}}(\omega) = \left(\frac{1}{2\pi} \int_{-\infty}^{\infty} \frac{\mathrm{d}k_1}{D_{\omega,k_1} + \chi_{\text{eq}}^{\text{h-s}}(\omega, k_1)} \right)^{-1}. \tag{26}$$

Since the denominator of the integrand in Eq. (26) has no real zeros (due to the material damping in the half-space) and tends to zero at large $|k_1|$ proportionally to $|k_1|^{-4}$, Eq. (26) can be readily integrated numerically.

The results of numerical integration are presented in Fig. 5, which shows the real and the imaginary parts of $\chi_{\mathrm{eq}}^{\mathrm{beam}}$ as functions of the radial frequency ω for five velocities of the oscillator. A low frequency band $\omega < 40$ rad/s is shown in the figure, since for higher frequencies, which correspond to shorter waves, the assumption that the stresses are uniformly distributed beneath the beam is not valid. The solid and dashed lines in this figure correspond to the real and imaginary parts of $\chi_{\mathrm{eq}}^{\mathrm{beam}}$, respectively. The parameters used in calculations are shown in Table 1.

Fig. 5a shows that if the oscillator moves slowly as compared to the shear wave speed in the half-space the real part of the dynamic stiffness slightly decreases with frequency because of growing effect of inertia.

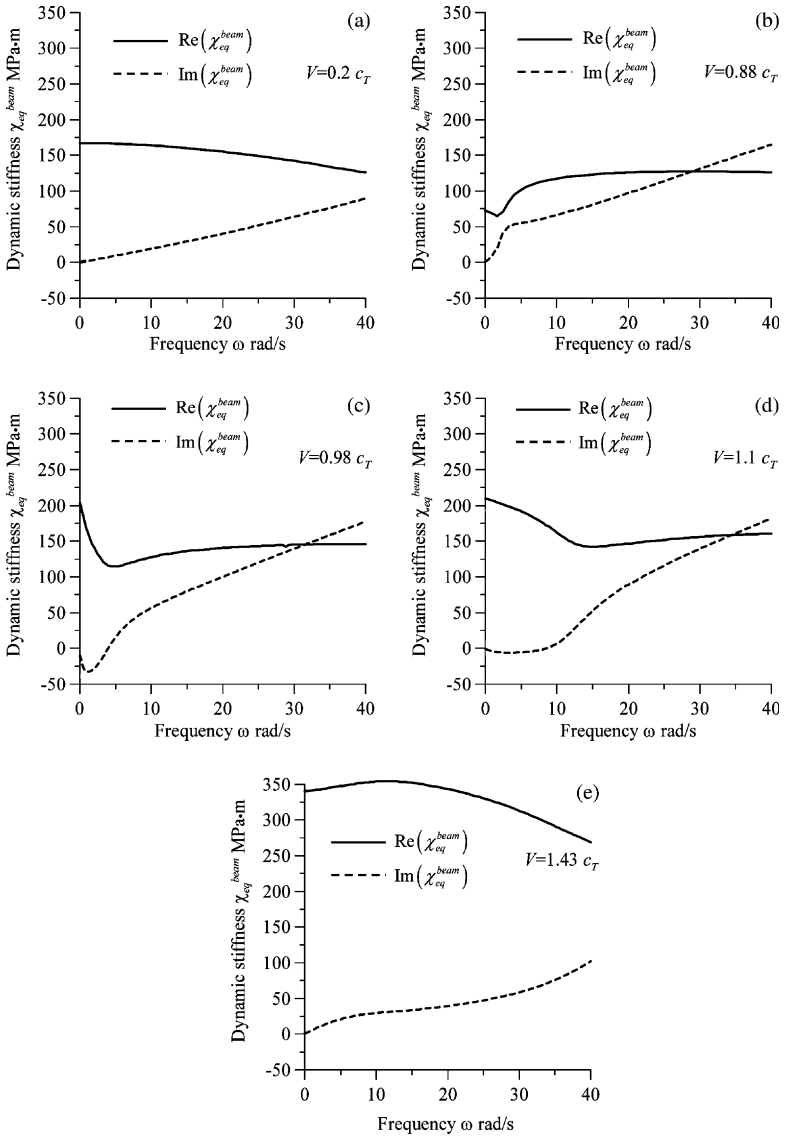

Fig. 5. The dynamic stiffness of the beam on the half-space versus the radial frequency of the oscillator for different velocities of the oscillator.

Table 1
Basic parameters of the system

Basic parameters				
Half-space			Beam+interface	Oscillator
$\nu = 0.3$	$\mu = 2.1 \times 10^7$ N/m^2	$\rho = 1960$ kg/m^3	EI $= 1.3 \times 10^8$ N/m^2	$M = 2 \times 10^4$ kg
$\mu^*/\mu = 10^{-4}$ s	$\lambda^*/\lambda = 10^{-4}$ s		$m_b = 7500$ kg/m	$m = 2 \times 10^3$ kg
$c_R = 95.9$ m/s	$c_T = 103.5$ m/s	$c_L = 193.6$ m/s	$a = 1.5$ m, $K = 0$	$\varepsilon = 0$

The imaginary part of the stiffness grows almost linearly in correspondence with the Kelvin–Voigt model for the material damping. This linear growth implies that the radiation damping plays no role in this case.

Fig. 5b corresponds to the oscillator's velocity, which is still lower than the Rayleigh wave speed in the half-space but higher than the minimum phase speed of the bending waves in the beam. This means that the oscillator can excite the bending waves in the beam even in the case that the frequency of its vibration is equal to zero. Consequently, at the very low frequency band, both the real and imaginary parts of the dynamic stiffness vary significantly because of excitation of waves in the beam. Despite of this variation, both parts remain positive, like in the previous case.

Fig. 5c corresponds to the oscillator's velocity, which is higher than the Rayleigh-wave speed but lower than the shear wave speed in the half-space. A crucial difference between this figure and the previous ones is that the imaginary part of the dynamic stiffness is negative in the low-frequency band (a "negative damping"). As shown by Metrikine and Dieterman (1997a), Metrikine and Popp (1999) and Verichev and Metrikine (2000) this implies that the vertical vibration of the oscillator may become unstable. To enable the dynamic stiffness to have a negative imaginary part and, consequently, to enable instability, there should be an external source, which supplies the beam-half-space system with energy. As shown by Metrikine (1994) this energy is supplied by the external source, which maintains the uniform motion of the oscillator along the beam. The work of this source is transferred into the energy of the vertical vibrations of the beam and the oscillator by so-called *anomalous Doppler waves*, whose properties are described in detail by Ginzburg (1990).

In Fig. 5d the velocity of the oscillator is slightly greater than the shear wave speed. The figure shows that the frequency band, corresponding to the negative imaginary part of the dynamic stiffness expands towards higher frequencies but the absolute value of $\mathrm{Im}(\chi_{\mathrm{eq}}^{\mathrm{beam}})$ decreases at this band.

If the velocity of the oscillator is increased further, $\mathrm{Im}(\chi_{\mathrm{eq}}^{\mathrm{beam}})$ becomes again positive at all frequencies as depicted in Fig. 5e. The stabilization factor, which removes the low-frequency "negative damping" is the material damping in the half-space. If the latter were absent, the imaginary part of the dynamic stiffness would be still negative at this oscillator's velocity. Note, however, that depending on the material properties of the half-space, the ratio of the oscillator's velocity and the shear wave speed, at which the "negative damping" disappears, can vary significantly. Moreover, for some parameters, $\mathrm{Im}(\chi_{\mathrm{eq}}^{\mathrm{beam}})$ can become negative again at a higher velocity than that shown in Fig. 5e.

In general, the stabilizing effect of the material damping in the half-space can be found at any velocity of the oscillator. As shown in Fig. 6a, in which $\mathrm{Im}(\chi_{\mathrm{eq}}^{\mathrm{beam}})$ is plotted for two magnitudes of the material damping for $V = 0.98c_T$, an increase of the material damping leads to a perceptible shrinkage of the frequency band at which the damping is "negative". In general, there always exists a magnitude of the material damping, which would ensure the system's stability for all velocities of the oscillator.

Another factor that influences the dynamic stiffness of the beam is the stiffness of the shear springs at the beam - half-space interface. As shown in Fig. 6b, once this stiffness is increased, the band with the "negative damping" expands and the value of $\mathrm{Im}(\chi_{\mathrm{eq}}^{\mathrm{beam}})$ in this band grows. This implies that increasing the shear stiffness of the interface, the system gets destabilized.

Concluding this section, let us point out its main result: the dynamic stiffness of the beam on the visco-elastic half-space can have a negative imaginary part (at a low frequency band), which can be interpreted as

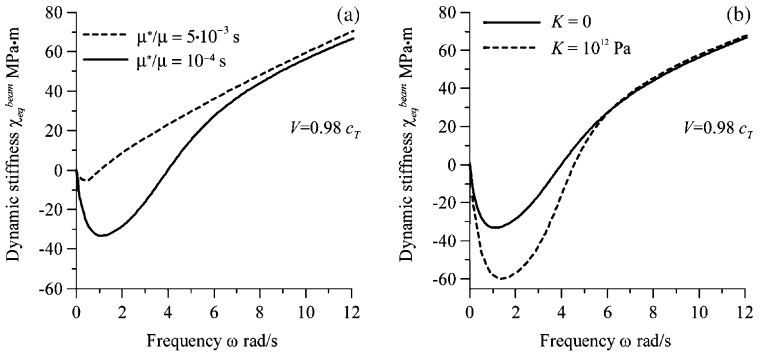

Fig. 6. The dynamic stiffness of the beam versus frequency: (a) effect of the material damping and (b) effect of the shear stiffness K.

a negative damping. The frequency band, in which $\mathrm{Im}(\chi_{\mathrm{eq}}^{\mathrm{beam}}) < 0$, as well as the magnitude of $\mathrm{Im}(\chi_{\mathrm{eq}}^{\mathrm{beam}})$ in this band, is strongly influenced by the material damping and affected by the stiffness of the shear springs at the beam—half-space interface. This implies that analyzing the system stability, the effect of these two factors should be thoroughly investigated.

4. The instability domain

Existence of a frequency band, in which the equivalent stiffness of the beam is negative, is a necessary but not a sufficient condition of instability (Metrikine and Verichev, 2001). To draw a conclusion on the system's stability, the roots of the characteristic equation Eq. (25) have to be studied. This study will be accomplished here with the help of the D-decomposition method, developed by Neimark (1978). The D-decomposition method utilizes the fact that the stability of a linear system is fully determined by the sign of the real part of its eigenvalues s. The eigenvalues, which correspond to unstable vibrations are located in the right half-plane of the complex s-plane. Consequently, the imaginary axis of this plane, $\lambda = \mathrm{i}\omega$, $\omega \in \mathbb{R}$ is the boundary that separates the "stable" and "unstable" eigenvalues (roots with $\mathrm{Re}(s) < 0$ and $\mathrm{Re}(s) > 0$, respectively). Assume now that the characteristic equation contains a parameter P that can be expressed explicitly. Such an expression can be then used as a mapping rule to map the imaginary axis of the s-plane onto the complex plane of the parameter P. The frequency ω serves as the parameter of this mapping. The resulting mapped line(s), which are referred to as D-decomposition line(s), will break the P-plane into domains with different number of "unstable" eigenvalues. Within a domain, this number may not vary.

Shading the right side of the imaginary axis of the s-plane (the side of "unstable" eigenvalues), and keeping the shading at the corresponding side of the D-decomposition line(s), the information contained in the decomposed P-plane can be enriched. With this shading, it becomes known that passing through a D-decomposition line in the direction of the shading corresponds to the gain of one additional "unstable" eigenvalue by the characteristic equation. Thus, if the number of the "unstable" eigenvalues is known for just one (arbitrary) value of the parameter P, the D-decomposed P-plane allows to draw a conclusion on stability of the system for all admissible values of this parameter at once.

Let us firstly carry out the stability analysis for a particular case, assuming that $M = K_0 = \varepsilon_0 = 0$ so that instead of the two-mass oscillator, a single mass moves on a beam. In this case, it is customary to perform the D-decomposition of the m-plane. As follows from the characteristic equation (25), the mapping rule in the case at hand is determined by the following equation (s is replaced by $\mathrm{i}\omega$):

$$m = \frac{\chi_{\mathrm{eq}}^{\mathrm{beam}}(\omega)}{\omega^2}. \tag{27}$$

The D-decomposition of the m-plane is shown and analyzed in Appendix C. On the basis of this analysis, using the parameters from Table 1, the instability domain is found, which is shown in Fig. 7. This figure shows that the instability can occur within a finite interval of the mass' velocities. The presence of the velocity (approximately 140 m/s), which bounds the instability domain from the right is caused by the material damping in the half-space. Consistently, this velocity has not been found in the earlier studies, which either employed a beam on Kelvin foundation (Metrikine and Dieterman, 1997a,b; Zheng et al., 2000), a plate on Kelvin foundation (Kononov and de Borst, 2002) or a beam on a purely elastic half-space (Metrikine and Popp, 1999). Another indirect consequence of the material damping is that to cause instability the mass should be unrealistically high. Note, however, that this holds only in the case that the elasticity of the moving oscillator is neglected.

Consider now the stability of the moving oscillator, taking into account its masses, the spring and the dashpot. In this case, the stiffness k_0 of the oscillator will be used as the parameter for D-decomposition. Substituting $s = \mathrm{i}\omega$ into the characteristic equation (25), the following mapping rule onto the complex k_0-plane is obtained:

$$k_0 = -\mathrm{i}\varepsilon_0\omega + M\omega^2 \frac{\chi_{\mathrm{eq}}^{\mathrm{beam}}(\omega) - m\omega^2}{\chi_{\mathrm{eq}}^{\mathrm{beam}}(\omega) - M\omega^2 - m\omega^2}. \tag{28}$$

The D-decomposition of the k_0-plane is presented in Appendix C. On the basis of this decomposition, the instability domain is found, which is shown in Fig. 8 for the parameters defined in Table 1.

The figure shows that the oscillator is unstable within a bell-shaped domain (in the stiffness-velocity plane). The main difference between this instability domain and those found in the earlier studies is that it is bounded from the right. As mentioned above, the material damping in the half-space causes this effect. Note that the instability domain in Fig. 8 corresponds to the velocities, which can be easily reached by modern high-speed trains. Moreover, the magnitudes of the stiffness correspond to realistic values of the suspension stiffness of high-speed trains. Thus, it is tempting to say that the instability can be considered as a realistic threat for high-speed trains. Before making such a statement, however, let us perform a parametric study of the stability domain. In this study, the parameters defined in Table 1 will be employed with one of these parameters varied.

Effect of the material damping of the half-space. In Fig. 9(a), the instability domain is depicted for two magnitudes of the material damping in the half-space. This figure shows that the effect of an increase of the material damping can be twofold: while diminishing the instability zone towards small magnitudes of the oscillator's stiffness, this damping leads to an expansion of the domain towards higher velocities of the

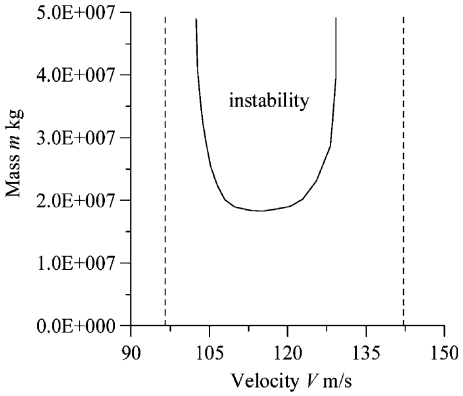

Fig. 7. Instability domain for a moving mass.

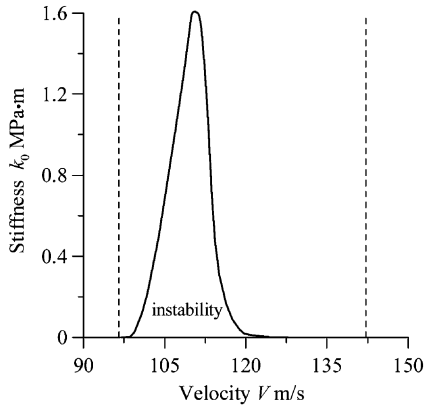

Fig. 8. Instability domain for a moving two-mass oscillator.

oscillator. Note that increasing the material damping further, it is always possible to reach a critical value, which would ensure the system's stability at any velocity of the oscillator. Thus, in general, the material damping stabilizes the system, although it can widen the instability zone with respect to the oscillator's velocity.

Effect of the Young's modulus of the half-space. In Fig. 9(b), the instability domain is presented for three magnitudes of the Young's modulus of the half-space. The figure shows that the instability zone shifts towards higher velocities and expands towards higher stiffness of the oscillator, as the half-space becomes stiffer. This implies that stiffening the ground, the critical velocity is increased but if this velocity is reached, the instability can arise in a wider range of parameters.

Effect of the shear springs at the interface. In Fig. 10, the instability domain is presented for two magnitudes of the shear stiffness: $K = 0$ and $K = 10^{12}$ Pa. This figure shows that the shear stiffness destabilizes the system leading to expansion of the instability zone in all directions. This implies that while making predictions on stability of high-speed trains, this stiffness should be accounted for.

Effect of the upper mass of the oscillator. Fig. 11(a), which presents the instability domain for three magnitudes of the upper mass, $M = 10^3$ kg, $M = 2 \cdot 10^3$ kg and $M = 3 \cdot 10^3$ kg, shows that this mass destabilizes the system leading to the zone expansion in all directions. This implies that heavier trains would experience the instability more likely.

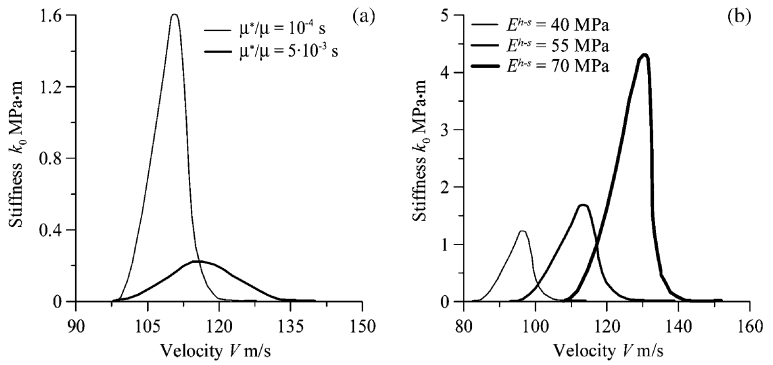

Fig. 9. Effect of parameters of the half-space: (a) material damping and (b) Young's modulus.

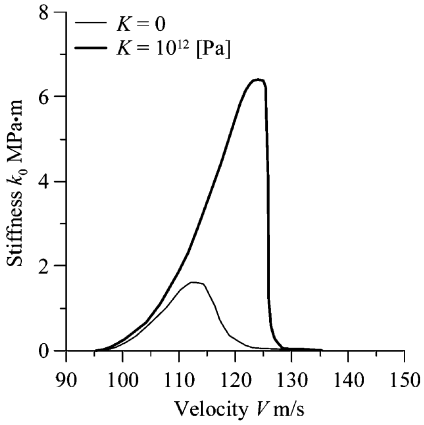

Fig. 10. Effect of the shear stiffness of the interface.

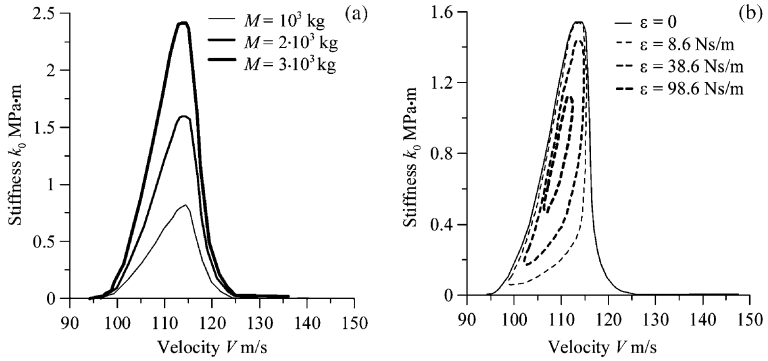

Fig. 11. Effect of parameters of the oscillator: (a) upper mass and (b) viscosity.

Effect of the viscosity of the oscillator. In Fig. 11(b), the instability domain is depicted for three magnitudes of the oscillator's viscosity: $\varepsilon_0 = 8.6$ N s/m, $\varepsilon_0 = 18.6$ N s/m and $\varepsilon_0 = 38.6$ N s/m. As follows from this figure, in contrast to the other parameters, the viscosity changes the instability zone not only quantitatively but qualitatively as well. An increase of the viscosity transforms the bell-shaped zone into an ellipse, which shrinks rapidly and then disappears. Thus, as well as the material damping of the half-space, the oscillator's viscosity can make the system unconditionally stable. However, the stabilization effect of the oscillator's viscosity is much stronger in the sense that even a relatively small (with respect to the critical) viscosity of the oscillator can remove the instability zone completely.

Formulating results of this section in practical terms, one can say that the easiest way to ensure the stability of a high-speed train is to introduce a sufficiently big viscosity in the bogies of the train. The analysis, carried out in this paper, shows that the viscosity, which would be needed to stabilize a train is smaller than that, used in the bogies of modern high-speed trains. Thus, the instability should not be expected in practice unless such factors as the thermo-induced compression of rails, unroundness of the train's wheels or curvature of the track would amplify it.

5. The instability in 3D and 1D models

In the engineering practice, the dynamics of railway tracks is normally modelled with the help of one-dimensional models. Therefore, it would be of practical relevance to know whether one-dimensional models can be used to predict the instability quantitatively correctly. In order to explore this, it is assumed that the beam is supported by a one-dimensional foundation instead of the half-space. This foundation is characterised by a mass m_f (kg/m), stiffness k_f (N/m^2), and two damping factors: $c_\mathrm{f}^{(1)}$ (N s/m^2) and $c_\mathrm{f}^{(2)}$ (N s), all parameters related to unit length. The mass m_f of the foundation is associated with a mass of the half-space, which vibrates together with the beam and can be referred to as the added mass. The stiffness of the foundation is introduced in accordance with the Winkler theory. The damping factors $c_\mathrm{f}^{(1)}$ and $c_\mathrm{f}^{(2)}$ are employed to describe the energy dissipation in the half-space. The first factor $c_\mathrm{f}^{(1)}$ is associated with the viscous part of this dissipation. Correspondingly, the differential operator $c_\mathrm{f}^{(1)}\partial_t$ describes dissipation that grows linearly with the frequency and is independent of the wavelength of the beam vibrations. The second factor $c_\mathrm{f}^{(2)}$ is associated with the part of dissipation that is of the 'internal friction' type. This type of dissipation depends both on the frequency and the wavenumber of the beam vibrations. Because of this, the effect of the 'internal friction' grows much faster with the frequency than that of the viscous damping.

The vertical motion of the beam on the above-described foundation under the moving oscillator is governed by the following equation:

$$((m_\mathrm{b}+m_\mathrm{f})\partial_{tt}+EI\partial_{xxxx}+c_\mathrm{f}^{(1)}\partial_t-c_\mathrm{f}^{(2)}\partial_{txx}+k_\mathrm{f})w^\mathrm{b}=-\delta(x-Vt)(md_{tt}w^{01}+(k_0+\varepsilon_0 d_t)(w^{01}-w^{02})). \quad (29)$$

Elaborating Eq. (29), Eqs. (4) and (5) in the same manner as described by Metrikine and Verichev (2001), the following characteristic equation can be obtained for the vertical vibrations of the oscillator:

$$(ms^2+k_0+s\varepsilon_0+\chi_\mathrm{1D}^\mathrm{beam}(s))(Ms^2+k_0+s\varepsilon_0)-(k_0+s\varepsilon_0)^2=0 \quad (30)$$

with

$$\chi_\mathrm{1D}^\mathrm{beam}(s)=\left(\frac{1}{2\pi}\int_{-\infty}^{\infty}\frac{\mathrm{d}k_1}{(m_\mathrm{b}+m_\mathrm{f})(s-\mathrm{i}k_1V)^2+EIk_1^4+(c_\mathrm{f}^{(1)}+k_1^2c_\mathrm{f}^{(1)})(s-\mathrm{i}k_1V)+k_\mathrm{f}}\right)^{-1}.$$

The characteristic equation (30) has exactly the same form as Eq. (25) and differs from the latter by the expression for the dynamic stiffness of the beam only.

Let us compare the instability zone, which is predicted by the 3D and 1D models. To this end, a correspondence should be established between the half-space parameters and those of the one-dimensional foundation in Eq. (29). Since the most conventional 1D-foundation is the Winkler foundation, which is characterised by the stiffness k_f, it is reasonable to start the identification of the foundation's parameters from this stiffness. An exact way to establish the correspondence between the stiffness k_f and the parameters of the half-space is to take the limit $s\to 0$ in the expression for the dynamic stiffness of the half-space, Eq. (22). However, even if this limit were calculated, Eq. (22) would still contain integrals over the wavenumber k_1, which would have to be evaluated numerically. This could be done but such an approach would diminish the main advantage of the 1D model: its simplicity. To keep this advantage, the stiffness k_f can be chosen more or less arbitrarily, not in correspondence with the parameters of the half-space but on the basis of experience (theoretical and practical), which says that this stiffness is in the order of 10^8 N/m^2.

Now that the magnitude of the stiffness k_f has been chosen, the mass per unit length of the foundation *must* be calculated in correspondence with the parameters of the half-space. It can be done by requiring that the minimum phase velocity of bending waves in the beam on the half-space and in the beam on the 1D foundation are the same. As shown by Dieterman and Metrikine (1996), the minimum phase velocity $V_\mathrm{3D}^\mathrm{min}$ of the beam on elastic half-space is slightly smaller than the Rayleigh wave speed c_R. To avoid unnecessary complications, the difference $c_\mathrm{R}-V_\mathrm{3D}^\mathrm{min}$ can be disregarded and $V_\mathrm{3D}^\mathrm{min}$ can be considered equal to c_R. For the

one-dimensional model (without damping), the minimum phase velocity V_{1D}^{min} can be expressed analytically to give

$$V_{1D}^{min} = \frac{(4EI k_f)^{1/4}}{\sqrt{m_b + m_f}}. \tag{31}$$

Imposing the requirement that $V_{1D}^{min} = V_{3D}^{min} = c_R$, the following expression for the mass per unit length of the one-dimensional foundation can be found:

$$m_f = -m_b + 2\frac{\sqrt{EI k_f}}{c_R^2} \approx 17295 \text{ kg}. \tag{32}$$

Eq. (32) shows that a significant "added mass" is involved in the motion of a beam on the half-space.

The remaining task is to define the damping factors $c_f^{(1)}$ and $c_f^{(2)}$. Let us first assume that $c_f^{(2)}$ equals zero and require the ratio $c_f^{(1)}/k_f$ be the same as the ratio $\mu^*/\mu = 10^{-4}$ s thereby unifying the ratio of the damping parameter and the elastic parameter in the models. The boundary of the instability zone, which corresponds to the chosen set of parameters of the 1D model ($k_f = 10^8$ N/m^2, $m_f = 17295$ kg, $c_f^{(1)} = 10^4$ N s/m^2) is shown in Fig. 12 by the dashed line. The instability zone is located on the right of this line.

Fig. 12 shows that the 1D model with $c_f^{(2)} = 0$ predicts reasonably well the left-hand-side boundary of the instability zone of the 3D model. However, the 1D-boundary (the dashed line) has a positive slope for all velocities and therefore cannot predict the right-hand-side boundary of the 3D-instability zone. It can be shown that this behavior of the 1D-boundary cannot be changed by varying the magnitude of the damping factors $c_f^{(1)}$ and $c_f^{(2)}$.

It is not difficult to understand why the 1D model does not predict the right-hand-side boundary of the 3D-instability zone. The reason is that this boundary is caused by a substantial increase of the radiation damping and, as a consequence, of the damping in the material, which accompany the increase of the oscillator's velocity. To account for this effect within the 1D model, the damping factors $c_f^{(1)}$ and $c_f^{(2)}$ should be considered velocity-dependent. Of course, there is an ambiguity in choosing this velocity-dependence, whose only known property is that it occurs as soon as the velocity of the oscillator V exceeds c_R and then grows with V, see Dieterman and Metrikine (1996). Following the concept of taking "an easy approach", we choose for the following dependence:

$$c_f^{(1)} = \alpha(V^2/c_R^2 - 1)H(V - c_R), \quad c_f^{(2)} = \beta(V^2/c_R^2 - 1)H(V - c_R). \tag{33}$$

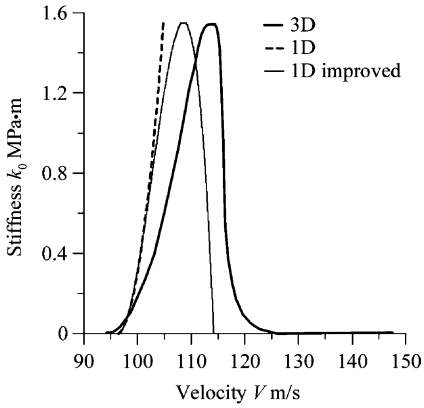

Fig. 12. The instability zone for 1D and 3D models.

Analysis shows that if $\beta = 0$ there is no way to chose the parameter α so that the 1D-instability zone would comply with the 3D-instability zone. On the contrary, keeping $\alpha = 0$, it is possible to find an appropriate value for the parameter β to find such compliance. The 1D-instability zone, which corresponds to $\alpha = 0$, $\beta = 2.28 \cdot 10^6$ N s is shown in Fig. 12 by the solid line, which is referred to as "1D improved".

Thus, we managed to find parameters of the 1D model so that the 3D-instability zone is predicted with a reasonable accuracy. However, to accomplish this, a tuning had to be done of the damping factors, which would be impossible if the 3D-instability zone were not known in advance. On this basis, one may conclude that 1D-models cannot be used for predicting the stability of a high-speed train.

6. Conclusions

In this paper, the stability of an oscillator that moves uniformly along a beam on a visco-elastic half-space has been studied. The beam on the half-space has been used as a simplistic three-dimensional model of a railway track, whereas the oscillator has been employed to model a bogie of a high-speed train.

The main goal of this paper has been to study the effect of the physical parameters of the system on the stability of the oscillator. The emphasis has been placed on the effect of the material damping of the half-space and the conditions at the beam-half-space interface. The second main goal has been to clarify whether one-dimensional models can be used for a quantitatively correct prediction of the stability of a high-speed train.

It has been shown that there exists a critical velocity of the oscillator that must be exceeded to enable the instability. As shown by Metrikine and Popp (1999) this velocity is always smaller than the Rayleigh-wave velocity if the half-space is purely elastic. With introduction of material damping according to the Kelvin–Voigt model, the critical velocity increases. Further, it has been found that there is a critical magnitude of the material damping that ensures the unconditional stability of the oscillator.

The main result of this paper is that the viscous damping of the oscillator (the viscosity of the bogie's suspension) in combination with the material damping in the half-space (the damping in the ground) stabilizes the system greatly. It has been shown that considering a realistic value for the material damping, introduction of a very small, about 200 N s/m, viscous damping of the oscillator stabilizes the system. This implies that the instability should not be considered as a real threat for high-speed trains, unless such factors as the thermo-induced compression of rails, unroundness of the train's wheels or curvature of the railway track would amplify it.

The second main result of this paper is the conclusion that one-dimensional models of railway tracks should not be used for quantitative prediction of the stability of high-speed trains. The reason is that there is no algorithm to determine effective parameters of a one-dimensional model so that the stability prediction would comply with that of a corresponding three-dimensional model.

Acknowledgements

This work has been partly supported by the Russian Foundation for Basic Research, grant 03-01-00644 and by Russian Science Support Foundation. This support is highly appreciated.

Appendix A

In the moving reference system, introduced by Eq. (6) the governing equations (1)–(5) read

- the equations of motion of the half-space

$$\tilde{c}_L^2\tilde{\nabla}^2\varphi = (\partial_\tau - V\partial_\xi)^2\varphi, \qquad \tilde{c}_T^2\tilde{\nabla}^2\boldsymbol{\psi} = (\partial_\tau - V\partial_\xi)^2\boldsymbol{\psi}, \qquad \tilde{\nabla}\bullet\boldsymbol{\psi} = 0 \tag{A.1}$$

with $\tilde{\nabla} = \xi_0\partial_\xi + y_0\partial_y + z_0\partial_z$, $\boldsymbol{\psi} = \xi_0\psi^\xi + y_0\psi^y + z_0\psi^z$,

- the balance of stresses at $z = 0$

$$\begin{aligned}
\sigma_{zz}(\tau,\xi,y,0) &= \frac{1}{2a}H(a-|y|)((m_{\mathrm{b}}(\partial_\tau - V\partial_\xi)^2 + EI\,\partial_{\xi\xi\xi\xi})w^{\mathrm{b}} \\
&\quad + \delta(\xi)(md_{\tau\tau}w^{01} + (k_0+\varepsilon_0 d_\tau)(w^{01}-w^{02}))), \\
\tau_{\xi z}(\tau,\xi,y,0) &= \frac{1}{2a}H(a-|y|)Ku(\tau,\xi,0,0), \\
\tau_{yz}(\tau,\xi,y,0) &= 0,
\end{aligned} \tag{A.2}$$

- the continuity of vertical displacements of the beam and the half-space:

$$w(\tau,\xi,0,0) = w^{\mathrm{b}}(\tau,\xi), \tag{A.3}$$

- the continuity of vertical displacements of the lower mass of the oscillator and the beam:

$$w^{01}(\tau) = w^{\mathrm{b}}(\tau,0), \tag{A.4}$$

- the equation of the vertical motion of the upper mass of the oscillator:

$$Md_{\tau\tau}w^{02} + (k_0+\varepsilon_0 d_\tau)(w^{02}-w^{01}) = 0. \tag{A.5}$$

For further evaluations, the displacements of the half-space and the surface tractions should be expressed in terms of the potentials φ and $\boldsymbol{\psi}$. Such expressions can be found in many textbooks, for example in the book of Achenbach (1973), and can be written as

$$u = \partial_\xi\varphi + \partial_y\psi^z - \partial_z\psi^y, \qquad v = \partial_y\varphi - \partial_\xi\psi^z + \partial_z\psi^\xi, \qquad w = \partial_z\varphi + \partial_\xi\psi^y - \partial_y\psi^\xi, \tag{A.6}$$

$$\begin{aligned}
\sigma_{zz} &= \tilde{\lambda}\nabla^2\varphi + 2\tilde{\mu}(\partial_{zz}\varphi + \partial_{\xi z}\psi^y - \partial_{yz}\psi^\xi) \\
\tau_{\xi z} &= \tilde{\mu}(2\partial_{\xi z}\varphi + \partial_{yz}\psi^z - \partial_{zz}\psi^y + \partial_{\xi\xi}\psi^y - \partial_{\xi y}\psi^\xi) \\
\tau_{yz} &= \tilde{\mu}(2\partial_{yz}\varphi + \partial_{zz}\psi^\xi - \partial_{\xi z}\psi^z + \partial_{\xi y}\psi^y - \partial_{yy}\psi^\xi)
\end{aligned} \tag{A.7}$$

Appendix B

The determinants in Eq. (17) are given as

$$\begin{aligned}
\Delta_0 &= R_T\frac{(s-\mathrm{i}k_1V)^2}{\tilde{c}_T^2}(q^2 - 4(k_1^2+k_2^2)R_LR_T), \\
\Delta_A &= -\mathrm{i}R_T\frac{(s-\mathrm{i}k_1V)^2}{\tilde{c}_T^2}(2k_1R_TH_\xi + \mathrm{i}qH_z), \\
\Delta_{B_\xi} &= -2k_2R_T\left(k_1H_\xi(q-2R_LR_T) - \mathrm{i}R_LH_z\frac{(s-\mathrm{i}k_1V)^2}{\tilde{c}_T^2}\right), \\
\Delta_{B_y} &= R_T\left((4k_2^2R_LR_T + q(2k_1^2-q))H_\xi - 2ik_1R_LH_z\frac{(s-\mathrm{i}k_1V)^2}{\tilde{c}_T^2}\right), \\
\Delta_{B_z} &= -\mathrm{i}k_2H_\xi(q^2 - 4(k_1^2+k_2^2)R_LR_T), \quad \text{with } q = k_1^2+k_2^2+R_T^2.
\end{aligned} \tag{B.1}$$

Appendix C

The D-decomposition of the m-plane, which is governed by Eq. (27), can have two qualitatively different patterns. The first pattern corresponds to the case (sub-critical) that the imaginary part of the dynamic stiffness of the beam is positive at all frequencies, like it is shown in Figs. 5a, b and e. In this case, considering as an example $V = 0.88c_T$ and using the parameters given in Table 1, the m-plane is decomposed as shown in Fig. 13(a). This figure shows that the D-decomposition curves do not cross the positive part of the real axis, implying that the stability of the system does not depend on the magnitude of the mass. Taking into account that no instability may occur as $m \to 0$, one should conclude that independently of the mass magnitude, the system is stable at this velocity.

The second pattern corresponds to the case (super-critical) that there exists a frequency band in which $\mathrm{Im}(\chi_{\mathrm{eq}}^{\mathrm{beam}}) < 0$, like it is shown in Fig. 5c and d. This pattern is shown in Fig. 13(b) for $V = 1.1c_T$. This figure shows that in the super-critical case the D-decomposition curves cross the positive part of the real axis. The position of this point is $m^* \approx 2.3 \times 10^6$ kg. Using again the fact that the system must be stable as $m \to 0$ and employing the direction of shading, a conclusion can be drawn that the instability occurs in the system if $m > m^*$ (there are two "unstable roots" as indicated in the figure).

To find the boundary of the instability domain in the plane $\{m, V\}$, the dependence $m^*(V)$ should be found. This dependence is shown in Fig. 7.

The D-decomposition of the k_0-plane is governed by the mapping rule Eq. (28) and can have two qualitatively different patterns, which are shown in Fig. 14. To plot this figure, the parameters defined in Table 1 have been used.

Fig. 14 presents the D-decomposition in the sub-critical case $V = 0.88c_T$, whereas Fig. 14(b) shows that in the super-critical case $V = 1.1c_T$. In order to determine the number of the "unstable roots" in the domains of the decomposed k_0-plane, the following kind of reasoning can be used. Consider that the stiffness of the oscillator tends to infinity, e.g. $\mathrm{Re}(k_0) \to \infty$, $\mathrm{Im}(k_0) = 0$. In this case, the masses of the oscillator vibrate as one mass, which, in accordance with Table 1 has the value of $m + M = 22 \times 10^3$ kg. As follows from Fig. 7, which shows the instability domain for a moving mass, the vibrations of such a mass are stable. This implies that the point of the k_0-plane defined as $\mathrm{Re}(k_0) \to \infty$, $\mathrm{Im}(k_0) = 0$ corresponds to the stable vibrations as well. Employing this fact, it can be readily concluded that the oscillator's vibrations in the sub-critical case are stable independently of the oscillator's stiffness k_0, whereas the super-critically moving oscillator can be unstable if its stiffness is smaller than a critical one. The latter is defined by the crossing point of the D-decomposition curves with the positive part of the real axis of the k_0-plane. Thus, to find the boundary of the instability domain for the moving oscillator, the position of this point should be

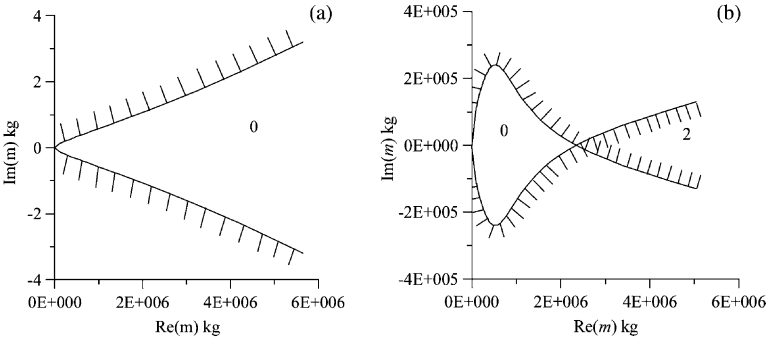

Fig. 13. D-decomposition of the m-plane: (a) sub-critical motion and (b) super-critical motion.

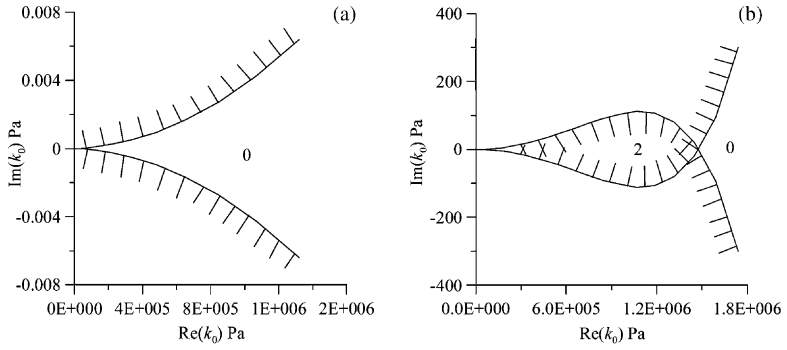

Fig. 14. D-decomposition of the k_0-plane: (a) sub-critical motion and (b) super-critical motion.

defined as a function of the oscillator's velocity. This function can be found numerically to give the instability domain, which is shown in Fig. 8.

References

Achenbach, J.D., 1973. Wave propagation in elastic solids. North-Holland Pub. Co., Amsterdam.

Andersen, L., Nielsen, S.R.K., Iwankiewicz, R., 2002. Vehicle moving along an infinite beam with random surface irregularities on a Kelvin foundation. ASME Journal of Applied Mechanics 69 (1), 69–75.

Andersen, L., Nielsen, S.R.K., 2003a. Boundary element analysis of the steady-state response of an elastic half-space to a moving force on its surface. Engineering Analysis with Boundary Elements 27 (1), 23–38.

Andersen, L., Nielsen, S.R.K., 2003b. Vibrations of a track caused by variation of the foundation stiffness. Probabilistic Engineering Mechanics 18 (2), 171–184.

Bogacz, R., Nowakowski, S., Popp, K., 1986. On the stability of a Timoshenko beam on an elastic foundation under a moving spring–mass system. Acta Mechanica 61, 117–127.

Clouteau, D., Degrande, G., Lombaert, G., 2001. Numerical modelling of traffic induced vibrations. Meccanika 36 (4), 401–420.

Denisov, G.G., Kugusheva, E.K., Novikov, V.V., 1985. On the problem of the stability of one-dimensional unbounded elastic systems. Journal of Applied Mathematics and Mechanics 49, 533–537.

Dieterman, H.A., Metrikine, A.V., 1996. The equivalent stiffness of a half-space interacting with a beam. Critical velocities of a moving load along the beam. European Journal of Mechanics A/Solids 15, 67–90.

Dieterman, H.A., Metrikine, A.V., 1997. Steady-state displacements of a beam on an elastic half-space due to a uniformly moving constant load. European Journal of Mechanics A/Solids 16, 295–306.

Filippov, A.P., 1961. Steady-state vibrations of an infinite beam on an elastic half-space under moving load. Izvestija AN SSSR OTN Mehanica and Mashinostroenie 6, 97–105 (in Russian).

Ginzburg, V.L., 1990. Applications of Electrodynamics in Theoretical Physics and Astrophysics. Gordon and Breach, New York.

Grundmann, H., Lenz, S., 2003. Nonlinear interaction between a moving SDOF system and a Timoshenko beam/halfspace support. Archive of Applied Mechanics 72 (11–12), 830–842.

Grundmann, H., Lieb, M., Trommer, E., 1999. The response of a layered half-space to traffic loads moving along its surface. Archive of Applied Mechanics 69, 55–67.

Kaynia, A.M., Madhus, C., Zackrisson, P., 2000. Ground vibration from high-speed trains: prediction and countermeasure. Journal of Geotechnical Geoenvironmental Engineering 126 (6), 531–537.

Kononov, A.V., de Borst, R., 2002. Instability analysis of vibrations of a uniformly moving mass in one and two-dimensional elastic systems. European Journal of Mechanics A/Solids 21, 151–165.

Krylov, V.V., 1995. Generation of ground vibrations by superfast trains. Applied Acoustics 44, 149–164.

Labra, J.J., 1975. An axially stressed railroad track on an elastic continuum subjected to a moving load. Acta Mechanica 22, 113–129.

Metrikine, A.V., 1994. Unstable lateral oscillations of an object moving uniformly along elastic guide as a result of anomalous Doppler effect. Acoustical Physics 40, 85–89.

Metrikine, A.V., Dieterman, H.A., 1997a. Instability of vibrations of a mass moving uniformly along an axially compressed beam on a viscoelastic foundation. Journal of Sound and Vibration 201, 567–576.

Metrikine, A.V., Dieterman, H.A., 1997b. Resonance interaction of vertical-longitudinal and lateral waves in a beam on a half-space. Journal of Applied Mechanics—Transactions of ASME 64, 951–956.

Metrikine, A.V., Popp, K., 1999. Instability of vibrations of an oscillator moving along a beam on an elastic half-space. European Journal of Mechanics A/Solids 18, 679–701.

Metrikine, A.V., Verichev, S.N., 2001. Instability of vibration of a moving two-mass oscillator on a flexibly supported Timoshenko beam. Archive of Applied Mechanics 71, 613–624.

Metrikine, A.V., Vesnitsky, A.I., 1996. Instability of vibrations of a mass moving uniformly over periodically and randomly-inhomogeneous elastic systems. ZAMM 76 (S4), 441–444.

Metrikine, A.V., Vostroukhov, A.V., Vrouwenvelder, A.C.W.M., 2001. Drag experienced by a high-speed train due to excitation of ground vibrations. International Journal of Solid and Structures 38, 8851–8868.

Neimark, Y.I., 1978. Dynamic Systems and Controllable Processes. Nauka, Moscow (in Russian).

Popp, K., Kruse, H., Kaiser, I., 1999. Vehicle-track dynamics in the mid-frequency range. Vehicle System Dynamics 31, 423–464.

Sheng, X., Jones, C.J.C., Petyt, M., 1999. Ground vibration generated by a load moving along a railway track. Journal of Sound and Vibration 228 (1), 129–156.

Verichev, S.N., Metrikine, A.V., 2000. Dynamic rigidity of a beam in a moving contact. Journal of Applied Mechanics and Technical Physics 41, 1111–1117.

Verichev, S.N., Metrikine, A.V., 2002. Instability of a bogie moving on a flexibly supported Timoshenko beam. Journal of Sound and Vibration 253, 653–668.

Verichev, S.N., Metrikine, A.V., 2003. Instability of vibrations of a mass that moves uniformly along a beam on a periodically inhomogeneous foundation. Journal of Sound and Vibration 260, 901–925.

Vostroukhov, A.V., Metrikine, A.V., 2003. Periodically supported beam on a visco-elastic layer as a model for dynamic analysis of a high-speed railway track. International Journal of Solids and Structures 40 (21), 5723–5752.

Zheng, D.Y., Au, F.T.K., Cheung, Y.K., 2000. Vibration of vehicle on compressed rail on viscoelastic foundation. ASCE Journal of Engineering Mechanics 126, 1141–1147.

Zheng, D.Y., Fan, S.C., 2002. Instability of vibration of a moving-train-and-rail coupling system. Journal of Sound and Vibration 255, 243–259.